Supporting information

Photocatalytic and sonocatalytic degradation of EDTA and Rhodamine B over Ti⁰ and Ti@TiO₂ nanoparticles

Sara El Hakim, Tony Chave, Sergey I. Nikitenko*

ICSM, Univ Montpellier, UMR 5257, CEA-CNRS-UM-ENSCM, Marcoule, France

Correspondence: serguei.nikitenko@cea.fr (S.N.); Tel.: +33-04 66 33 92 51 (S.N.)
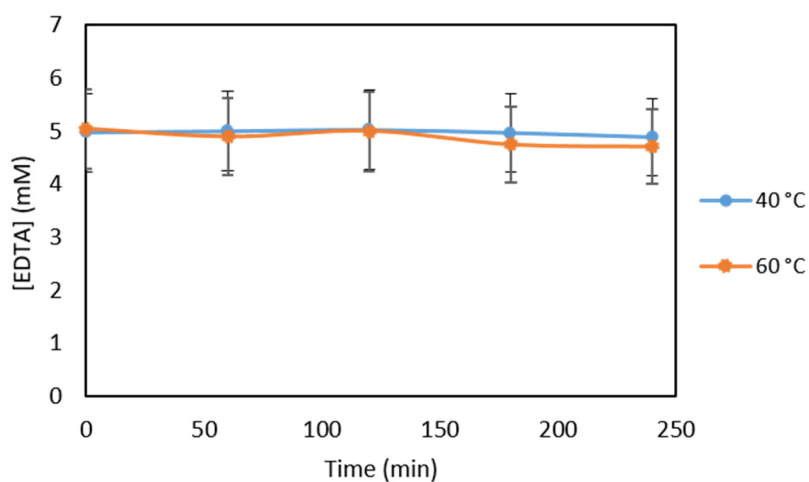
Figure S1.   Kinetic curves of EDTA evolution during photolysis of 5 mM initial EDTA solutions under Ar atmosphere at 40 and 60 °C in the presence of Ti@TiO₂ NPs (catalyst concentration 0.12 g.L^{-1}, V = 65 mL, P_{light} = 9.5 W).
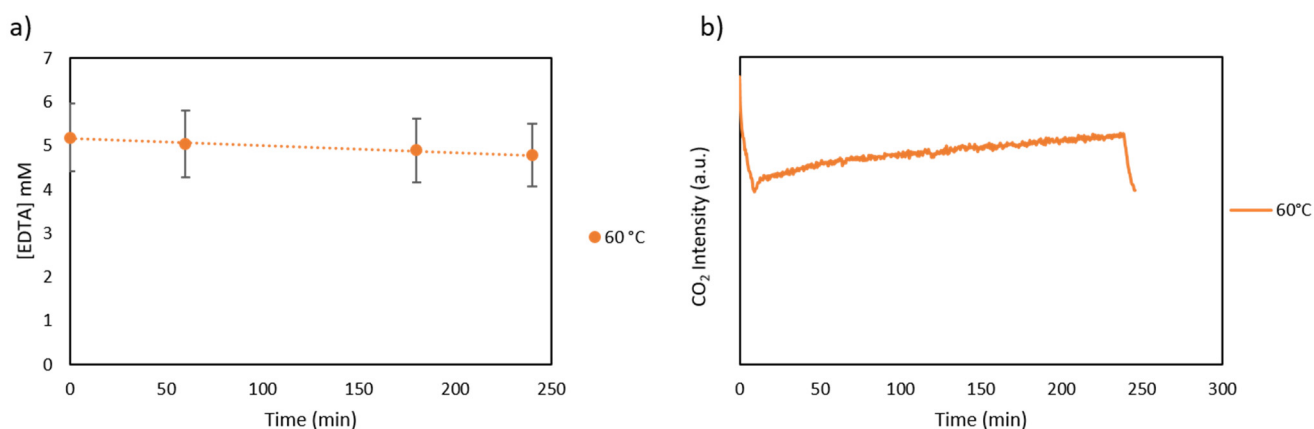

Figure S2.   Kinetic curves of EDTA evolution (a) and CO_2 emission profile (b) during photolysis of 5 mM initial EDTA solutions under Ar20%O₂ atmosphere at 60 °C in the presence of Ti⁰ NPs (catalyst concentration 0.12 g.L^{-1}, V = 65 mL, P_{light} = 9.5 W).
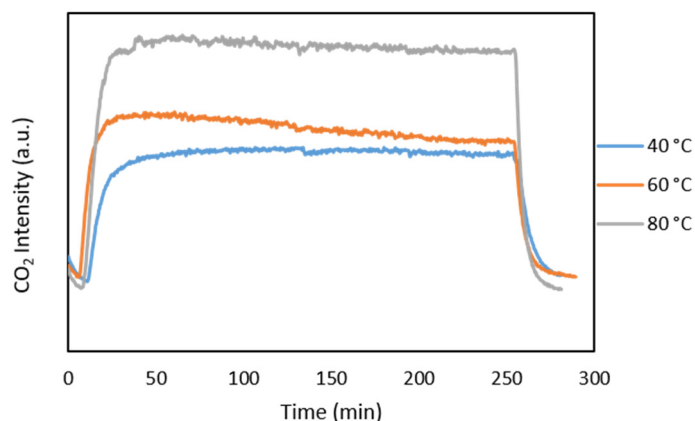
Figure S3.   Typical carbon dioxide emission profiles obtained upon irradiating 5 mM EDTA solution under the white light of the Xe lamp and in the presence of Ti@TiO$_2$ catalyst under Ar20%O$_2$ (catalyst concentration 0.12 g.L^{-1}, V = 65 mL, P$_{Xe\ light}$ = 9.5 W).

As shown in Figure S4, the background signal of the CO$_2$ emission profiles released once operating under Ar atmosphere posses an unstable background. Therfore, the, CO$_2$ yield at 40 °C was not possibly calculated and that at 60 °C varied from 35 to 25 ± 10% µmol.kJ^{-1}.g^{-1} which is ca.6 times smaller than the one obtained under same condition but with Ar20%O$_2$ (128 ± 13 µmol.kJ^{-1}.g^{-1}) as presented in Figure 1.
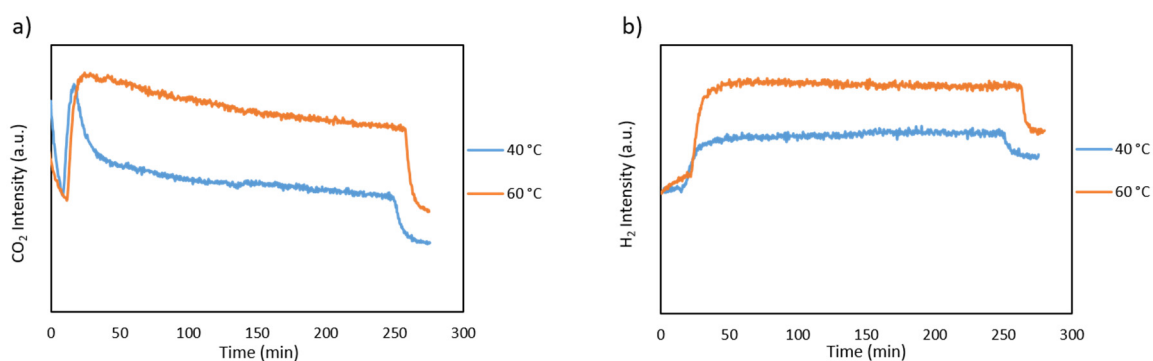

Figure S4.   Typical carbon dioxide (a) and hydrogen(b) emission profiles obtained upon irradiating 5 mM EDTA solution under the white light of the Xe lamp and in the presence of Ti@TiO$_2$ catalyst under Ar (catalyst concentration 0.12 g.L^{-1}, V = 65 mL, P$_{Xe\ light}$ = 9.5 W).
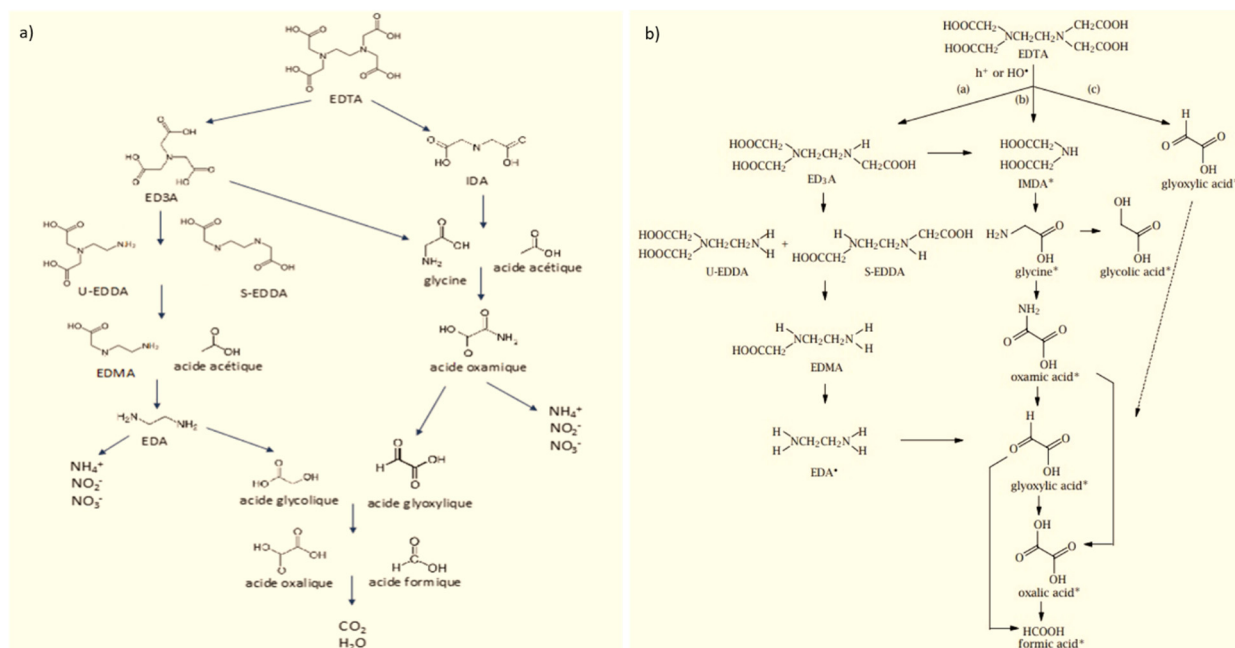
Figure S5.   By-products of sonocatalytic [21] (a) and photocatalytic [15] (b) EDTA degradation.
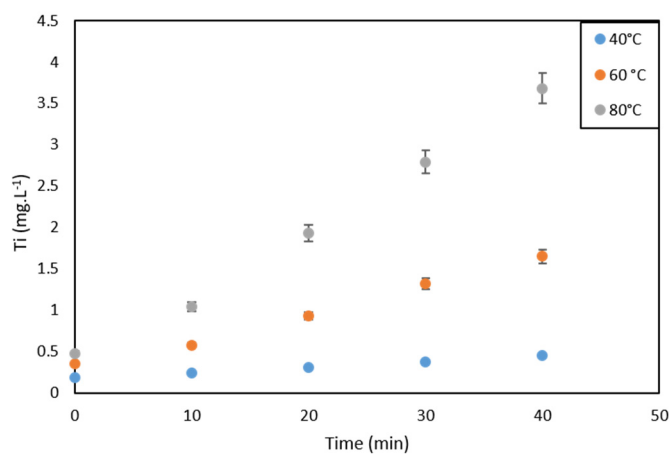

Figure S6. Evolution of titanium concentration in solution during photocatalytic experiments with 0.25 M H_2SO_4 solutions over Ti@TiO$_2$ NPs at different temperatures in the presence of Ar/20%O$_2$ (catalyst concentration 2 g L^{-1}, V= 65 mL). Concentration of titanium was measured by ICP-OES technique after Ti@TiO$_2$ NPs removal using PTFE filter.
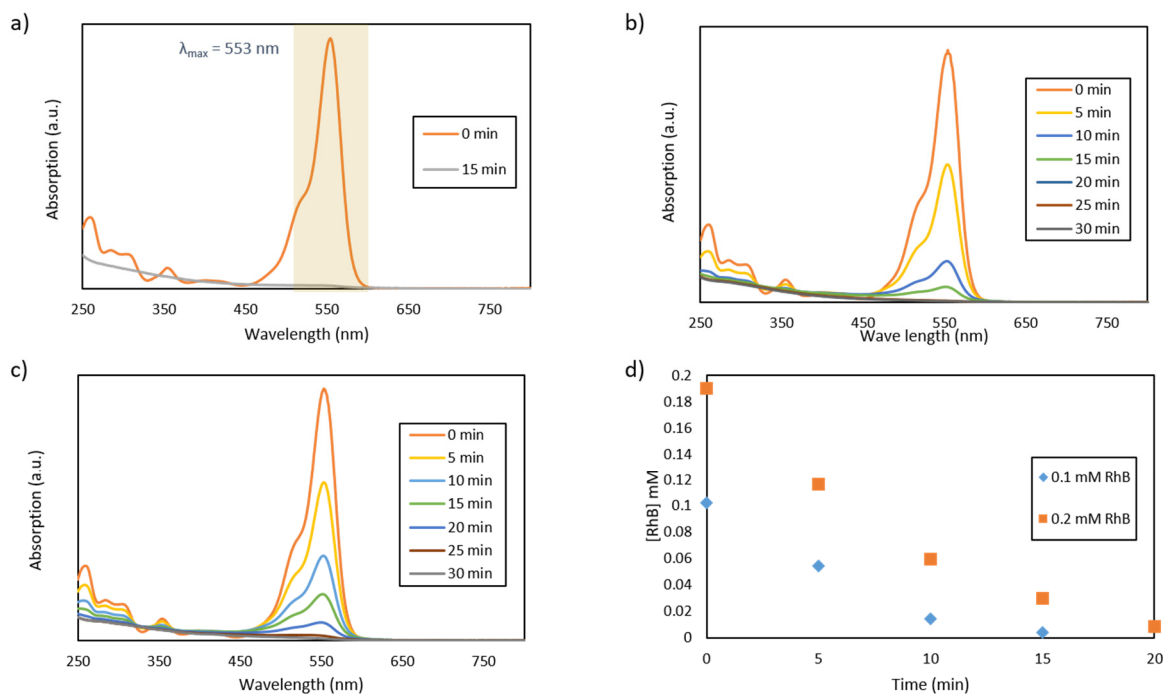
Figure S7.   Absorption spectrum of 10^{-2} mM (a), 10^{-1} mM (b) and $2 \cdot 10^{-1}$ mM (c) RhB solution during sonolysis at 40 °C with 345 kHz in Ar20%O$_2$. Major absorption peak of RhB is at 553 nm. [RhB] degradation profiles as a function of time 10^{-1} and $2 \cdot 10^{-1}$ mM are shown in graph (d).
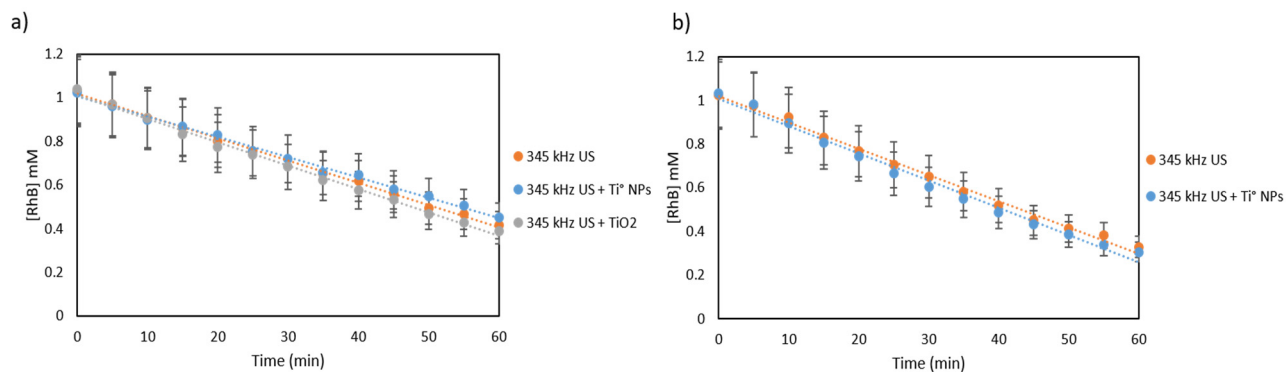

Figure S8.   Kinetics of RhB evolution upon ultrasonic treatment under Ar (a) and under Air (b) flux in the presence of solid particles (catalyst concentration 0.4 g L^{-1}, T = 40 °C).
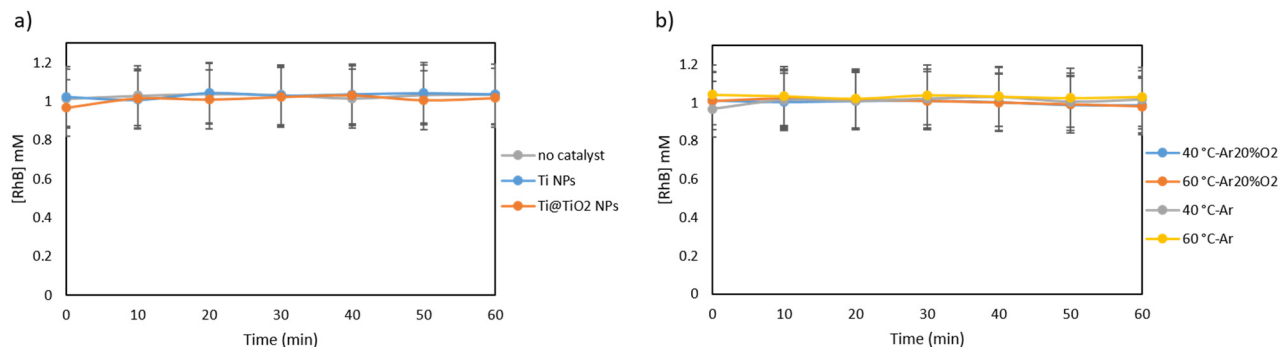
Figure S9. Variation of RhB concentraion upon photothermal treatment of 1 mM RhB solution with and without catalyst under Ar flux at 40 °C (a) and with Ti@TiO$_2$ at 40 °C and 60 °C with Ar and Ar/20%O$_2$ (catalyst concentration 0.12 g L^{-1}, V$_{RhB}$= 60 mL).
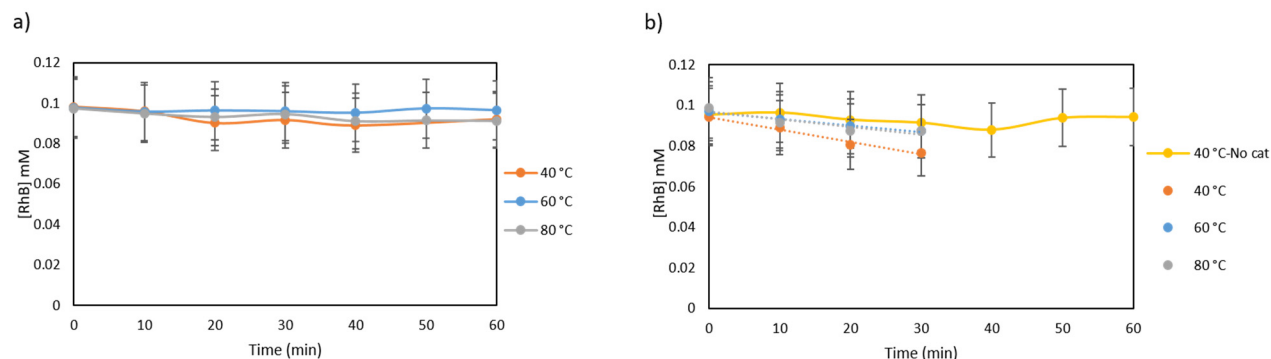

Figure S10. Variation of RhB concentraion upon photothermal treatment of 0.1 mM RhB solution with Ti@TiO$_2$ catalyst under Ar (a) and under Ar/20%O$_2$ (b) (catalyst concentration 0.12 g L^{-1}, V$_{RhB}$= 60 mL).
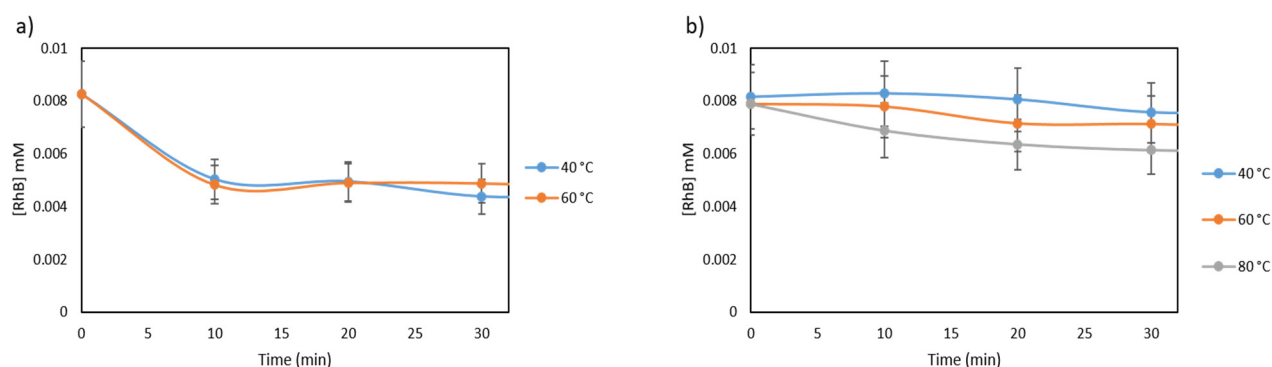

Figure S11. Variation of 0.01 mM initial RhB concentration upon photocatalytic treatment with Ti@TiO$_2$ under Ar atmosphere (a) and with Ti^0 under Ar/20%O$_2$ atmosphere (b) (catalyst concentration 0.12 g^{-1}.L^{-1}).
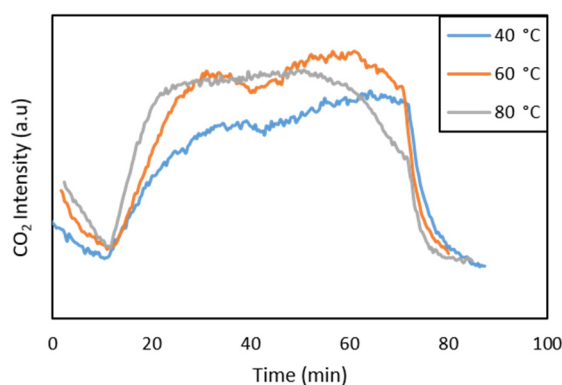

Figure S12. Carbon dioxide emission profiles from photothermal treatment of 0.01 mM RhB solutions in the presence of Ti@TiO$_2$ photocatalyst under Ar/20%O$_2$ atmosphere at 40, 60 and 80 °C (catalyst concentration 0.12 g^{-1}.L^{-1} V = 65 mL, P$_{Xe\ light}$ = 9.5 W).
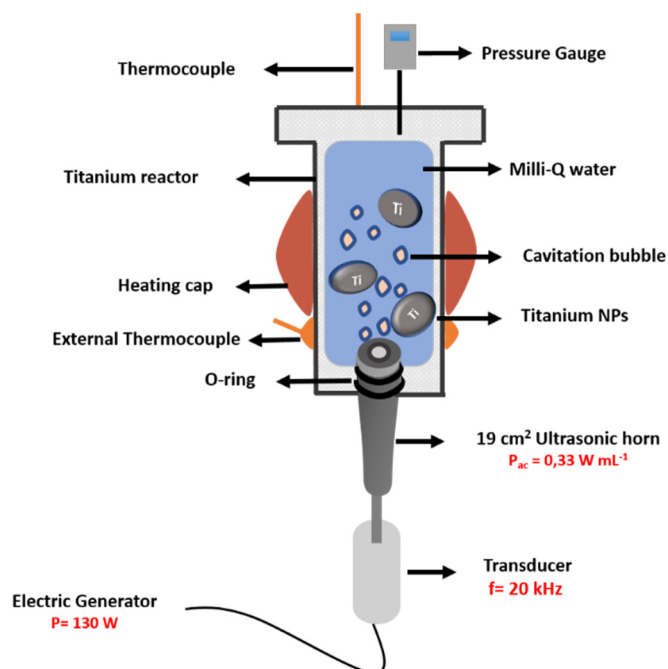
Figure S13. Graphical sketch of sonohydrothermal reactor

The sonohydrothermal reactor was made from Ti-6Al-4V titanium alloy and equipped with a 19 cm² commercial ultrasonic horn made from the same alloy and powered by a 20 kHz piezoelectric transducer and an electric generator (130 W SONICS). The ultrasonic horn was tightly fitted in the bottom part of the reactor using O-rings made from Aflas® 75 rubber (ERIKS). Temperature control was provided by a removable heater fitted on the external surface of the vessel with two thermocouples inside and outside the reactor. Both thermocouples and the heater were connected to VULCANIC 30 656 control panel. The pressure inside the vessel was measured using calibrated digital manometer. Ultrasonic transducer was cooled with air flow. The absorbed acoustic power was measured at near-room temperature using thermal probe method (Mason T. J., Lorimer J. P. *Applied Sonochemistry. The Uses of Power Ultrasound in Chemistry and Processing*, Wiley-VCH, Weinheim, **2002**).
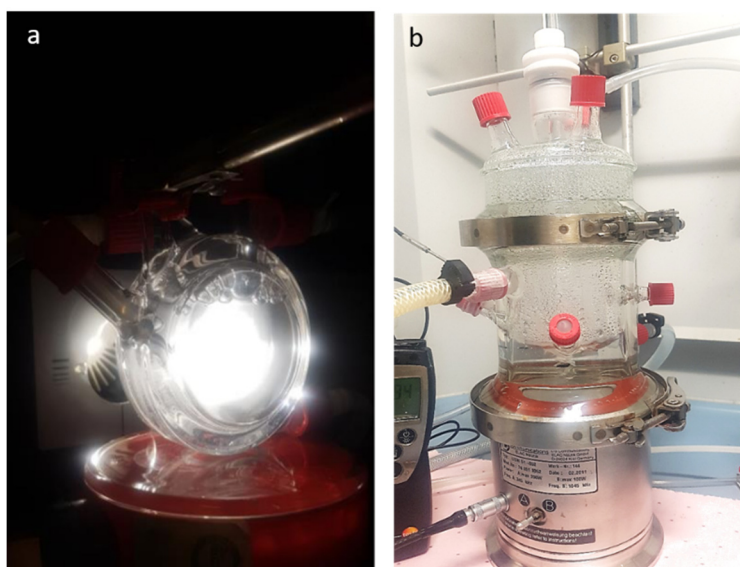

Figure S14. Images of the thermostated photocatalytic cell (a) and the high frequency sonochemical reactor (b).